

A Hybrid Density Functional-Classical Molecular Dynamics Simulation of a Water Molecule in Liquid Water

Iñaki Tuñón [a,b], Marilia Teresa C. Martins-Costa [a], Claude Millot [a] and Manuel F. Ruiz-López [a,*]

[a] Laboratoire de Chimie théorique-UA CNRS 510 (Institut Nancéien de Chimie Moléculaire), Université Henri Poincaré, Nancy I, B.P. 239, 54506 Vandoeuvre-lès-Nancy Cedex, France (*ruiz @ lctm.u-nancy.fr*)

[b] Departamento de Química Física, Universidad de Valencia, 46100 Burjasot (Valencia), Spain

Received: 18 July 1995 / Accepted: 25 September 1995

Abstract

A hybrid NVE Molecular Dynamics simulation of liquid water is presented using a coupled Density Functional/Molecular Mechanics hamiltonian. The quantum subsystem is a single water molecule described by means of a triple-zeta quality basis set with polarization orbitals on oxygen and hydrogen atoms. Non-local exchange-correlation corrections are included self-consistently. The classical system is constituted by 128 TIP3P water molecules. Results are in reasonable agreement with experimental data and in particular a good description of the solute polarization is obtained. Large fluctuations of the instantaneous value of the dipole moment of the quantum molecule are predicted.

Keywords: Computer Simulations, QM/MM Potentials, Density Functional Theory, Molecular Dynamics, Liquid Water.

Introduction

Solute-solvent interactions play a fundamental role in many chemical processes such as equilibria and reactions [1]. The development of liquid models allowing the study of solvated system properties has received much attention in recent years. Two main approaches have been considered: continuum models [2] and statistical simulations [3]. The former lead to an efficient implementation into quantum treatments combining an oversimplified model for the solvent, which is simply characterized by a dielectric constant, with a detailed electronic description of the solute. In the statistical methods such as Monte Carlo or Molecular Dynamics, a great number of solvent molecules can be considered but the use of a simplified interaction potential, even with explicit introduction of the polarizability in the model, cannot give a

very accurate description of the electronic structure of the solute when chemical reactions are involved.

Recently, much effort has been devoted to the development of hybrid models that combine some of the advantages of the two previous approaches. These hybrid models consist in the statistical treatment of a large system, enzyme or solution for instance, in which a small part is studied at the quantum mechanical level (QM) and the bulk system is described through molecular mechanics potentials (MM) [4-8]. This approach allows the investigation of polarization effects and reactive processes in solution as well as a good description of the solvent structure. Because of the extensive computational effort needed to carry out these simulations, the quantum part has been usually modelled by means of a semiempirical hamiltonian [4-6]. This semiempirical QM/MM approach has been implemented both in Monte Carlo and Molecular Dynamics obtaining very promising results.

* To whom correspondence should be addressed

However, semiempirical methods are not always accurate enough and one may need to carry out ab initio calculations. In principle, extension of the QM/MM approach to ab initio methods is possible but the computing time would be too large especially considering that the calculation of the correlation energy is required to describe many chemical phenomena. As an alternative, Density Functional Theory (DFT) techniques, which have been remarkably improved over the last few years [9], are very promising. DFT results have been shown to reproduce hydrogen bonds and cooperative effects in solution correctly [10-12] provided that non-local corrections to the exchange-correlation energy are included. Recent calculations have shown that the use of coupled DFT/MM potentials can be employed successfully in the study of solvation processes [7,8,13,14]. In a previous paper [8], we have described the implementation of DFT/MM potentials into a Monte Carlo algorithm and results for liquid water [8] and aqueous solutions of several ions [14] have been reported. In this paper, we describe the implementation of the hybrid potential in Molecular Dynamics. Besides, an improved DFT/MM potential is used to describe a DFT water molecule in liquid water.

Description of the model

The total energy of the system can be divided into three components: the energy of the subsystem described quantum mechanically (dft), the energy of the system described at the classical mechanical level (mm) and the interaction between the DFT and the MM portions (dft/mm):

$$E(R_n, R_s) = E_{dft}(R_n) + E_{mm}(R_s) + E_{dft/mm}(R_n, R_s) \quad (1)$$

where R_n is the position of the quantum mechanical nuclei and R_s the position of the solvent interaction sites. Both E_{dft} and $E_{dft/mm}$ terms depend on the electronic density of the quantum subsystem $\rho(r)$ obtained from the solution of the corresponding Kohn-Sham equations[15] :

$$\left[-\frac{\hbar^2}{2m} \nabla^2 - \left(\sum_n \frac{eZ_n}{r_{in}} + \sum_s \frac{eq_s}{r_{is}} \right) + \int dr' \frac{\rho(r')}{|r-r'|} + \frac{\delta E_{xc}}{\delta \rho(r)} \right] \Psi_i(r) = \epsilon_i \Psi_i(r)$$

$$\rho(r) = \sum_i \Psi_i(r) \Psi_i(r) \quad (2)$$

Here, Ψ_i is the molecular orbital of electron i and E_{xc} is the exchange-correlation functional.

Once the electronic density of the quantum subsystem has been determined for a given configuration of solute and sol-

vent molecules, the different energy parts can be computed as follows:

$$E_{dft}(R_n) = -\frac{\hbar^2}{2m} \int dr \sum_i \Psi_i(r) \nabla^2 \Psi_i(r) + \int dr \sum_n \frac{Z_n}{|R_n - r|} \rho(r) + \frac{1}{2} \iint dr dr' \frac{\rho(r) \rho(r')}{|r-r'|} + E_{xc}[\rho(r)] + \sum_n \sum_{n' > n} \frac{Z_n Z_{n'}}{r_{nn'}} \quad (3)$$

$$E_{dft/mm}(R_n, R_s) = \int dr \sum_s \frac{q_s}{|R_s - r|} \rho(r) + \sum_{n,s} \frac{q_s Z_n}{r_{sn}} + \sum_{s,n} 4\epsilon_{sn} \left[\left(\frac{\sigma_{sn}}{r_{sn}} \right)^{12} - \left(\frac{\sigma_{sn}}{r_{sn}} \right)^6 \right] \quad (4)$$

The last term of $E_{dft/mm}$ is the crossed van der Waals energy between quantum nuclei and solvent interaction sites. The molecular mechanics energy term is given by the classical equation:

$$E_{mm}(R_s) = \sum_{s,s'} \frac{q_s q_{s'}}{r_{ss'}} + \sum_{s,s'} 4\epsilon_{ss'} \left[\left(\frac{\sigma_{ss'}}{r_{ss'}} \right)^{12} - \left(\frac{\sigma_{ss'}}{r_{ss'}} \right)^6 \right] \quad (5)$$

where s and s' run over solvent sites of different molecules.

Analytical forces acting on DFT molecule nuclei (F_n) and MM solvent sites (F_s) are obtained from the derivatives of the energy with respect to their positions:

$$F_n = -\frac{\partial E(R_n, R_s)}{\partial R_n} \quad F_s = -\frac{\partial E(R_n, R_s)}{\partial R_s} \quad (6)$$

The practical implementation of the DFT/MM potential in a NVE Molecular Dynamics simulation has been made as follows :

- for a given solute and solvent configuration, the Kohn-Sham (eq. 2) is solved
- the total energy (eq. 1) and forces (eq. 6) are calculated
- the averaged quantities are updated and the new wave function is stored to be used at the next step as the SCF initial guess
- the equations of motion are solved using the RATTLE algorithm for the rigid quantum molecule [16] and a quaternion-based leap-frog algorithm due to Fincham [17-18] for the molecular mechanical molecules.

The process is repeated using the new positions of quantum nuclei and solvent molecules.

Computational Details

Molecular Dynamics simulations have been performed in a cubic box of side 15.6 Å with 128 TIP3P [19] water molecules and a DFT water molecule at 25° C using the NVE ensemble. Periodic boundary conditions and a cutoff distance of 7.6 Å have been applied for all classical-classical and classical-quantum interactions. The integration step used was 1 fs. Equilibration was carried out during 40 ps followed by averaging over 70 ps.

Table 1. Experimental and calculated properties of the water molecule in liquid water. Positions of peaks in Å, dipole moments in debye and solvation enthalpies in kcal/mol.

	Exp	DFT/MM	
		DZP[a]	TZP
RDF first peak			
O-O	2.88[b]	2.72	2.72
O-H	1.85[b]	1.80[c]	1.85[c]
		1.75[d]	1.70[d]
H-H	2.33[b]	2.38	2.36
RDF second peak			
O-O	4.50[b]	4.92	
O-H	3.27[b]	3.23[c]	3.23[b]
		3.13[d]	3.16[d]
H-H	3.84[b]	3.74	3.72
Dipole moment			
gas	1.85[e]	2.28	2.09
water	2.6[f]	2.89	2.77
$\Delta\mu$	0.75	0.61	0.68
ΔH_{sol}			
	-10.5[g]	-13.2	-10.4

[a] Hybrid DFT/MM Monte Carlo simulation using a double-zeta basis set [8].

[b] Ref. 23

[c] quantum oxygen-classical hydrogen

[d] quantum hydrogen-classical oxygen

[e] Ref 24

[f] In ice, Refs. 25 and 26

[g] Ref. 29

The geometry and the Lennard-Jones parameters of the DFT water molecule were those of the TIP3P water monomer ($d=0.9572$ Å, $a=104.52^\circ$). Kohn-Sham equations were solved using the VWN functional [20] with density gradient corrections [21] proposed by Becke for the exchange and Perdew for the correlation term. Numerical integration of the exchange-correlation contribution is computed on a MEDIUM grid [22]. The deMon program [22] has been used for the DFT calculations. The triple-zeta quality basis set with polarization functions H(41/1*) and O(7111/411/1*) [22], hereafter called TZP, has been used. Auxiliary basis sets used in the fitting of the charge density and the exchange-correlation potential were H(4;4) and O(4,3;4,3) [22].

A further refinement of the model could be achieved by rescaling the Lennard-Jones parameters used to compute the crossed van der Waals energy between quantum nuclei and solvent interaction sites (see equation 4) [8,13]. This has not been envisaged in the present work but will be considered in future papers.

Results and Discussion

The results of the Molecular Dynamics simulation with the TZP basis set are gathered in Table 1 together with experimental data [23] and the results of our previous hybrid Monte Carlo simulation. In the latter, we used a double-zeta quality basis set with polarisation functions H(41) and O(621/41/1) [22] (hereafter called DZP). The RDFs for oxygen-oxygen, oxygen-hydrogen and hydrogen-hydrogen are plotted in Figures 1, 2, and 3 respectively.

The first oxygen-oxygen peak of the DFT/MM RDF appears at a distance shorter than the experimental value (2.72 Å versus 2.88 Å). The position obtained in our previous simulation using the DZP basis set was the same. The coordination number obtained from integration of the calculated quantum oxygen-classical oxygen curve up to the first minimum is close to that obtained from the experimental RDF (4.7 and 4.4 respectively). In contrast with our previous simulation with the

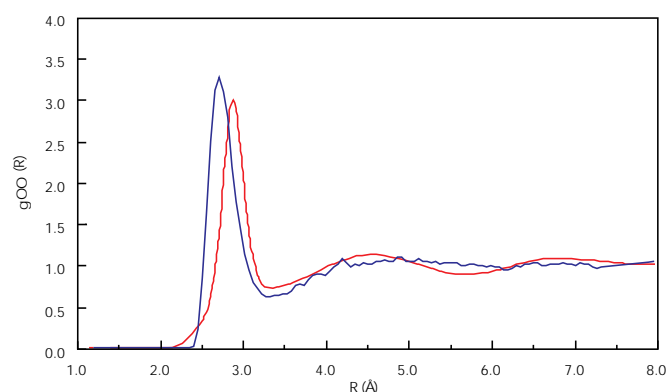


Figure 1. Oxygen-oxygen radial distribution functions: DFT/TIP3P (blue line) and experimental (red curve)

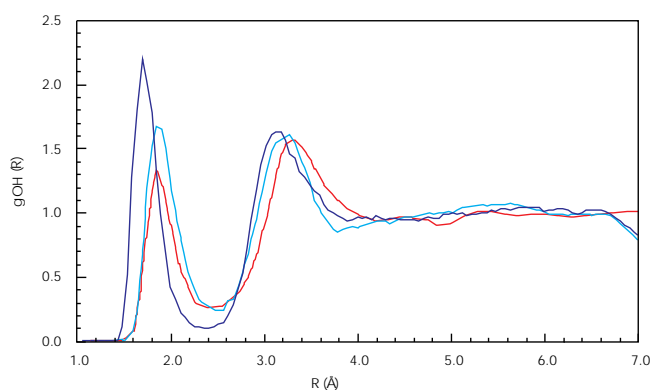


Figure 2. Oxygen-hydrogen radial distribution functions: DFT hydrogen-TIP3P oxygen (blue line), DFT oxygen-TIP3P hydrogen (cyan line) and experimental (red line).

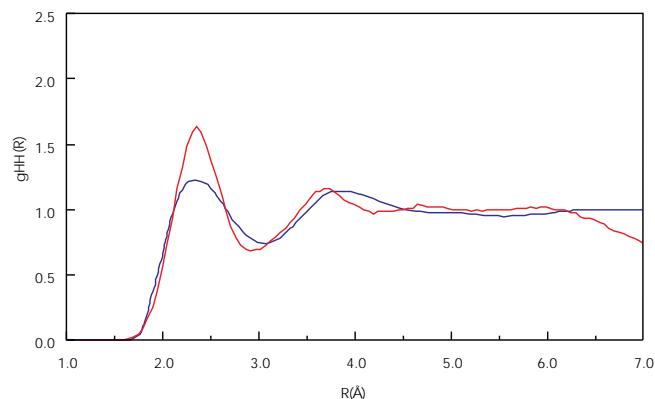


Figure 3. Hydrogen-hydrogen radial distribution functions. DFT/TIP3P (red line) and experimental (blue line).

DZP basis set, a second peak structure does not appear clearly in the oxygen-oxygen RDF. This could be attributed to a reduction of the interaction energy between the quantum and classical subsystems due to the lower value of the dipole moment predicted by the TZP basis set (see below).

Two different oxygen-hydrogen RDF curves have been obtained, one corresponding to the quantum oxygen-classical hydrogen and one to the quantum hydrogen-classical oxygen. As expected from our previous results [8], the quantum hydrogen-classical oxygen RDF peaks are more intense and appear at shorter distances than the quantum oxygen-classical hydrogen RDF ones. The minimum of the quantum hy-

drogen-classical oxygen RDF is deeper than the experimental one and than the minimum of the quantum oxygen-classical hydrogen RDF. The hydrogen-hydrogen RDFs are given in Figure 3. The DFT/MM RDF presents two well-located peaks with respect to the experimental curve, although the intensity of the first is larger than the experimental result. The first minimum is close in position and value to the experimental one.

The calculated dipole moments in gas phase and in solution are given in Table 1. The calculated gas phase dipole moment with the TZP basis set is slightly overestimated with

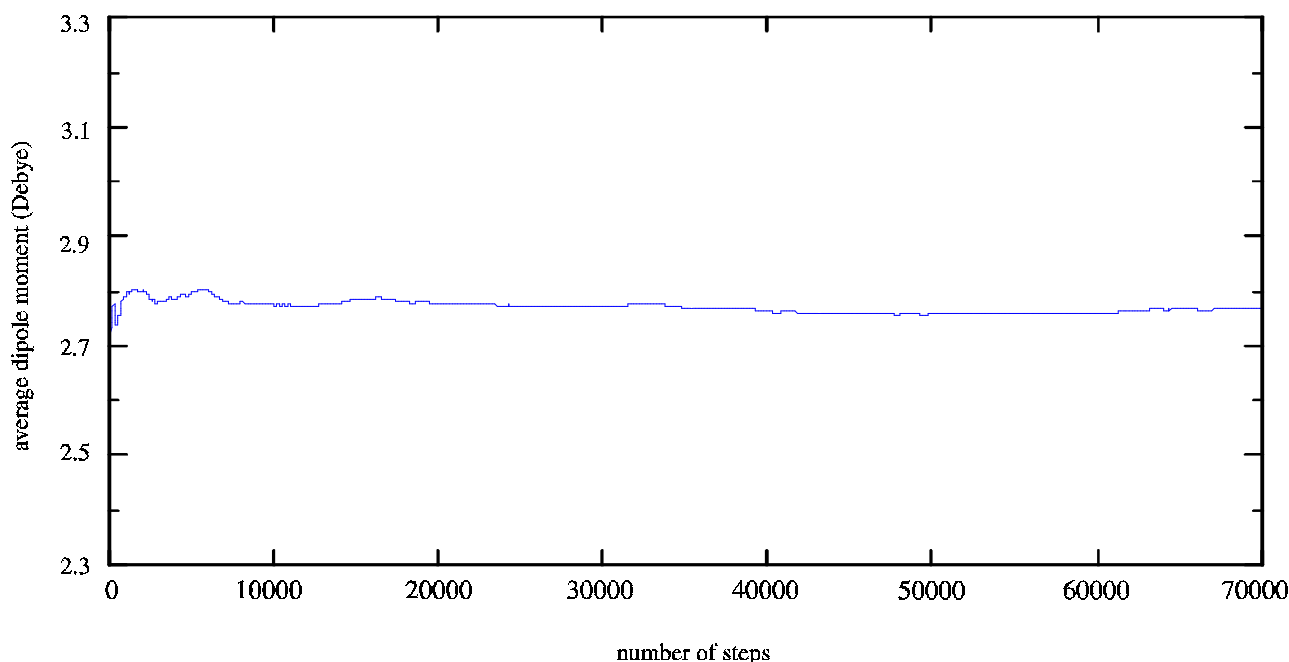


Figure 4. Cumulative average of the DFT water molecule dipole moment along the simulation.

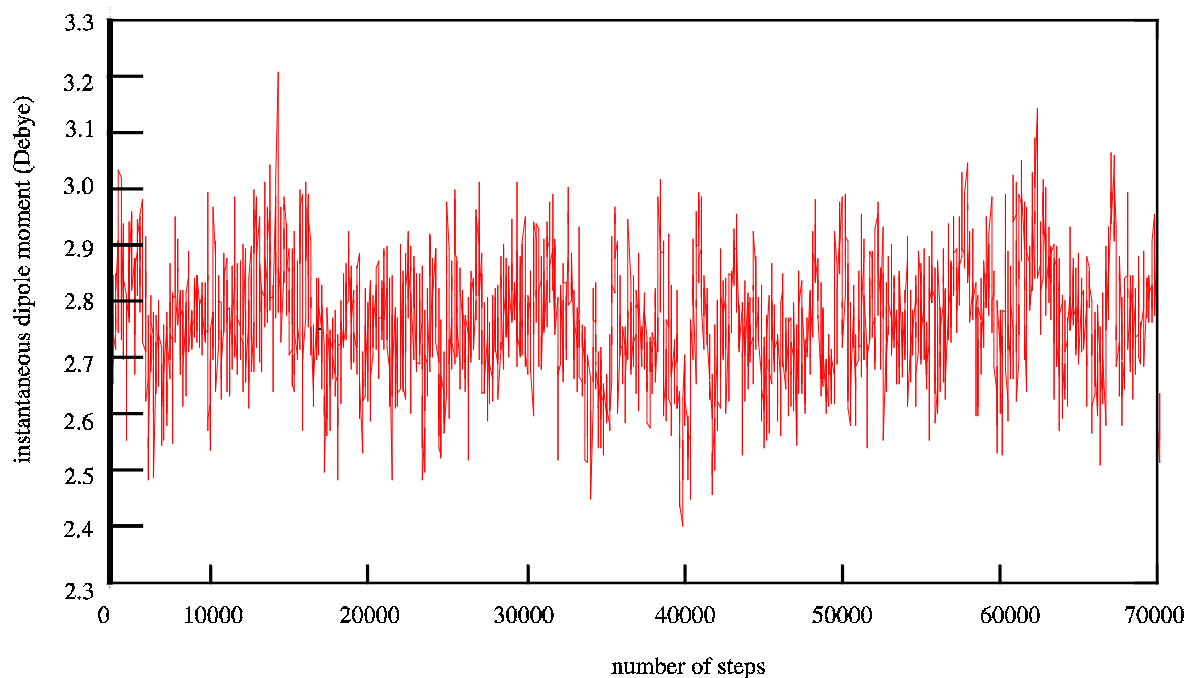


Figure 5. Instantaneous value of the DFT water molecule dipole moment along the simulation.

respect to the experimental value [24] (2.09 vs 1.85 D). The error in the calculated gas phase dipole moment with this basis set is considerably smaller than with the DZP basis set used in our previous work [8] (13% vs 23%). The greater flexibility of the TZP basis set, compared to the DZP basis set, is reflected in the larger averaged induced dipole moment obtained at the end of the simulation (0.68 D vs 0.61 D). This induced dipole moment is close to the experimental value estimated using the value in ice as the reference dipole moment in solution [25,26] (0.75 D). The resulting averaged dipole moment in solution obtained in our present hybrid MD simulation (2.77 D) is slightly larger than the experimental estimate for ice [25,26] (2.6 D) and than the result of a Car-Parrinello simulation of liquid water [27] (2.66 D). However, a considerable improvement is obtained with respect to the result obtained in the hybrid Monte Carlo simulation using the DZP basis set (2.89 D). One can expect to improve this agreement by using a larger basis set, in particular by including diffuse functions, since the gas phase dipole moment would be reduced [28] and the water polarizability would be increased.

The most interesting result of the hybrid MD simulation concerns the evaluation of the instantaneous polarization of the quantum molecule. In fact, large variations of the electronic density due to the movements of the liquid environment are predicted. In Figure 4 and 5 we present the averaged and instantaneous dipole moment of the DFT molecule along the 70000 steps of the simulation (70 ps) respectively. The dipole moment oscillates between 2.60 D and 3.0 D,

although it can occasionally reach smaller (2.4 D) and larger (3.2 D) values. Hence, one can estimate that the fluctuations of the charge density of a water molecule in liquid water may produce variations of ca. 0.2 D in the dipole moment with respect to its average value. These solvent-induced fluctuations of the solute electronic density are of primary interest in the analysis of chemical reactivity in solution since they may be at the origin of solvent-driven processes.

The solvation enthalpy of the quantum molecule (see Table 1) has been calculated as:

$$\Delta H_{sol} = \Delta U_{sim} - \Delta U_{liq} - E_{gas} - RT \quad (7)$$

where ΔU_{sim} is the total energy of the simulation, ΔU_{liq} is the energy of 128 TIP3P water molecules [19] and E_{gas} is the DFT energy of the water molecule in vacuo. The calculated solvation enthalpy in the hybrid MD simulation with the TZP basis set (-10.4 kcal/mol) is substantially closer to the experimental value [29] (-10.5 kcal/mol) than the result obtained in the hybrid Monte Carlo simulation with the DZP basis set (-13.2 kcal/mol) as could be expected from the analysis of the total dipole moment above. Finally, the averaged solute-solvent interaction energy is -28.0 kcal/mol.

Conclusions

A hybrid Molecular Dynamics algorithm has been implemented using a coupled DFT/MM hamiltonian. The water molecule in liquid water has been studied as a test case using triple-zeta quality basis sets with polarization functions and a non-local exchange-correlation potential. The computational scheme proposed leads to results for the radial dis-

tribution functions, solvation energy and solute polarization that are in good agreement with experimental data. In particular, the present calculations give a better description of polarization effects on the quantum molecule that in previous hybrid DFT/MM Monte Carlo simulations. Evaluation of the instantaneous value of the dipole moment of the quantum water molecule shows that the solvent can induced large fluctuations of the solute electronic density (± 0.2 D).

As far as the quantum calculations are carried out during the course of the simulation, this methodology appears to be very useful for analyzing reaction dynamics in solution. It is well known that the solvent may play a dynamic role in the case of some reactions such as electron or proton transfer processes in polar media. This dynamic effect is connected to non-equilibrium solvation and ultimately to the participation of the solvent on the reaction coordinate. The relation between solvent dynamic effects and solute charge fluctuations is an interesting field of research that can be raised with the help of hybrid models such as that described in this paper. Though these computations are still costly for medium size systems, the evolution of the hardware and the developing of parallel computing allows one to hope that simulations of experimentally interesting reactions will become a reality in near future.

Acknowledgments I. T. acknowledges the warm hospitality of all the members of the Laboratoire de Chimie Théorique a post-doctoral fellowship and a post-doctoral contract of the Ministerio de Educación y Ciencia (Spain). This work was partly supported by DGICYT Project PB93-0699.

References

- Reichardt, C. in *Solvents and Solvent Effects in Organic Chemistry*; VCH, Weinheim, **1988**.
- (a) Onsager, L. *J. Am. Chem. Soc.* **1936**, *58*, 1486; (b) Rivail, J. L.; Rinaldi, D. *Chem. Phys.* **1976**, *18*, 233; (c) Miertus, S.; Scrocco, E.; Tomasi, J. *Chem. Phys.* **1981**, *55*, 117; (d) Cramer, C. J.; Truhlar, D. G. *Science*, **1992**, *256*, 213.
- (a) Chandrasekhar, J.; Smith, S. F.; Jorgensen, W. L. *J. Am. Chem. Soc.* **1985**, *107*, 154; (b) Allen, M. P.; Tildesley, D. J. in *Computer Simulation of Liquids*, Oxford University Press, New York, **1987**; (c) McCammon, J. A.; Harvey, S. C. in *Dynamics of Proteins and Nucleic Acids*, Cambridge University Press, Cambridge, **1987**.
- (a) Warshel, A.; Levitt, M. *J. Mol. Biol.* **1976**, *103*, 227; (b) Warshel, A. *J. Phys. Chem.* **1979**, *83*, 1640; (c) Luzhkov, V.; Warshel, A. *J. Comp. Chem.* **1992**, *13*, 199.
- (a) Bash, P.; Field, M. J.; Karplus, M. *J. Am. Chem. Soc.* **1987**, *109*, 8092; (b) Field, M. J.; Bash, P. A.; Karplus, M. *J. Comp. Chem.* **1990**, *11*, 700.
- (a) Gao, J.; Xia, X. *Science* **1992**, *258*, 631; (b) Gao, J. *J. Phys. Chem.* **1992**, *96*, 537.
- Stanton, R. V.; Hartsough, D. S.; Merz Jr., K. M. *J. Phys. Chem.* **1993**, *97*, 11868.
- Tuñón, I.; Martins-Costa, M. T. C.; Millot, C.; Ruiz-López, M. F.; Rivail, J. L. *J. Comp. Chem.*, in press.
- Parr, R. G.; Yang, W. in *Density-Functional Theory of Atoms and Molecules*, Oxford University Press, New York, **1989**.
- Ruiz-López, M. F.; Bohr, F.; Martins-Costa, M. T. C.; Rinaldi, D. *Chem. Phys. Letters* **1994**, *221*, 109.
- Sim F.; St-Amant, A.; Papai, I.; Salahub, D. R. *J. Am. Chem. Soc.* **1992**, *114*, 4391.
- Mijoule, C.; Latajka, Z.; Borgis, D. *Chem. Phys. Letters* **1993**, *208*, 364.
- Stanton, R. S.; Hartsough, D. S.; Merz Jr., K. M. *J. Comp. Chem.* **1995**, *16*, 113.
- Tuñón, I.; Martins-Costa, M. T. C.; Millot, C.; Ruiz-López, M. F. *Chem. Phys. Letters* **1995**, *241*, 450.
- Kohn, W.; Sham, L. J. *Phys. Rev. A* **1965**, *140*, 1133.
- Andersen, H. C. *J. Comp. Chem.* **1983**, *52*, 24.
- Fincham, D. *CCP5 Quarterly*, **1981**, *2*, 6.
- Fincham, D.; Heyes, D.M. *Adv. Chem. Phys.*, **1985**, *68*, 493.
- Jorgensen, W. L.; Chandrasekar, J.; Madura, J. D.; Impey, R. W.; Klein, M. L. *J. Chem. Phys.* **1983**, *79*, 926.
- Vosko, S. H.; Wilk, L.; Nusair, M. *Can. J. Phys.* **1980**, *58*, 1200.
- Becke, A. D. *Phys. Rev. A* **1988**, *38*, 3098; Perdew, J. P. *Phys. Rev. B* **1986**, *33*, 8822; Perdew, J. P. *Phys. Rev. B* **1986**, *34*, 7406.
- (a) St-Amant, A.; Salahub, D. R. *Chem. Phys. Letters* **1990**, *169*, 387; (b) Salahub, D. R.; Fournier, R.; Mlynarski, P.; Papai, I.; St-Amant, A.; Ushio, J. in *Theory and Applications of Density Functional Approaches to Chemistry*, J. Labanowski and J. Andzelm Eds., Springer Verlag, Berlin **1991**.
- Soper, A. K.; Phillips, M. G. *Chem. Phys.* **1986**, *107*, 47.
- Clough, S. A.; Beers, Y.; Klein, G. P.; Rothman, L. S. *J. Chem. Phys.* **1973**, *59*, 2254.
- Coulson, C. A.; Eisenberg, D. *Proc. Roy. Soc. London A* **1966**, *291*, 445.
- Whalley, E. *Chem. Phys. Letters* **1978**, *53*, 449.
- Laasonen, K.; Sprik, M.; Parrinello, M.; Car R. *J. Chem. Phys.* **1993**, *99*, 9080.
- Wei, D.; Salahub, D. R. *Chem. Phys. Letters* **1994**, *224*, 291.
- Kell, G. S. *J. Chem. Eng. Data* **1975**, *20*, 97.